

# Methyl Hexadecyl Viologen Inclusion in Cucurbit[8]uril: Coexistence of Three Host–Guest Complexes with Different Stoichiometry in a Highly Hydrated Crystal

Neal Hickey, Barbara Medagli, Alessandro Pedrini, Roberta Pinalli, Enrico Dalcanale, and Silvano Geremia\*



Cite This: *Cryst. Growth Des.* 2021, 21, 3650–3655



Read Online

ACCESS |



Metrics & More

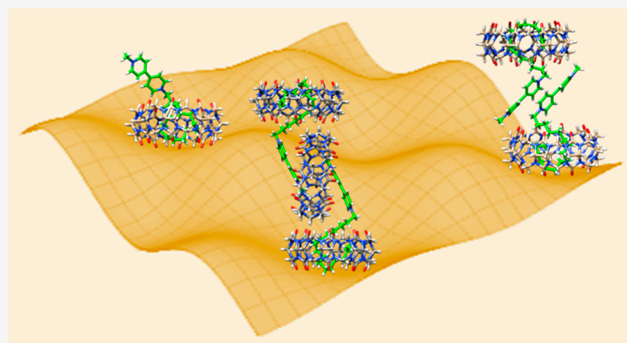


Article Recommendations



Supporting Information

**ABSTRACT:** The host–guest inclusion complexes of cucurbiturils with alkyl viologen have interesting architectures, chemical properties, and potential applications in sensors and nanotechnology. A highly hydrated triclinic crystal of cucurbit[8]uril (CB[8]) complexed by methyl hexadecyl viologen (MVC16) is characterized by the unprecedented coexistence in the crystal of three host–guest complexes with 3:2, 2:2, and 1:1 stoichiometries. In all these complexes, the hook-shaped alkyl chain of the MVC16 is hosted in the CB[8] macrocycles, while the methyl viologen moieties have various environments. In the Z-shaped 3:2 complex, a central CB[8] unit hosts two viologen heads in the cavity, while the 2:2 complex is held together by  $\pi$ -stacking interactions between two viologen units. In the square 2D tiling crystal packing of CB[8] macrocycles, the same site which favors the dimerization observed in the 2:2 complex is also statistically occupied by a single methyl viologen moiety of the 1:1 complex. The rational interpretation of the crystal structure represented an intriguing challenge, due to the complicated statistical disorder in the alkyl chains hosted in CB[8] units and in the methyl viologen moieties of 2:2 and 1:1 complexes. In contrast with the solution behavior dominated by the 2:1 complex, the coexistence of three host–guest complexes with 3:2, 2:2, and 1:1 ratios highlights the fundamental importance of packing effects in the crystallized supramolecular complexes. Therefore, the crystallization process has permitted us to capture different host–guest systems in a single crystal, revealing a supramolecular landscape in a single photo.



Cucurbit[ $n$ ]urils (CB[ $n$ ]), composed of  $n$  glycoluril units cyclically connected by  $2n$  methylene linkers, represent an interesting example of versatile host molecules in supramolecular chemistry.<sup>1–5</sup> These highly symmetric pumpkin-shaped molecules have a hydrophobic hollow cavity and two rimmed polar ureido carbonyl openings, the sizes of which increase as  $n$  increases.<sup>1</sup> In fact, the various CB[ $n$ ]'s have the same depth (9.1 Å), but their annular widths and equatorial widths vary systematically from CB[5] to CB[10]. The two symmetric portals range from 2.4 Å in CB[5] to more than 10 Å in CB[10].<sup>1</sup> Within this family, the CB[8] molecules are a good compromise for the host–guest properties, because their 6.9 Å portals can accommodate in the cavity aromatic molecules as well as long aliphatic alkyl chains in a U-folded conformation.<sup>6</sup> Furthermore, more propensity to crystallize is shown with respect to the odd-numbered cucurbiturils.<sup>7</sup> This remarkable macrocyclic structure represents a well preorganized platform for sensor development, nanotechnology, and biomimetic chemistry.<sup>4,8–10</sup> A large number of host–guest inclusion complexes of CB[ $n$ ] with interesting architectures, chemical properties, and potential applications have been

reported.<sup>8,11–14</sup> Among these supramolecular complexes, viologen compounds are special guest molecules in CB[8] chemistry, as they can develop strong and specific host–guest interactions which can be chemically, photochemically, or electrochemically controlled.<sup>15–17</sup> Furthermore, the interaction with CB[8] can be modulated by the presence of alkyl substituents with various chain lengths on the viologen guest, which can significantly change its complexation mode and the stoichiometry of the supramolecular complex that can be formed.<sup>18</sup> It should be noted that complexes of CB[8] have in general a less predictable stoichiometry, owing to its larger cavity compared to the smaller CB[5], CB[6], and CB[7] members. In fact, it has been observed that CB[8] has the

Received: April 21, 2021

Revised: May 26, 2021

Published: May 28, 2021



ability to form 1:1 binary,<sup>18</sup> 2:1 and 1:2 ternary,<sup>6,19</sup> 2:2 quaternary,<sup>20</sup> and 3:2 quinary<sup>21</sup> complexes with various viologen derivatives, as well as  $n:n$  oligomers<sup>8</sup> and  $2n:n$  host–guest<sup>22</sup> supramolecular polymers.

Recently, we have reported a thorough study of the influence of the alkyl chain length on the binding mode of methyl alkyl viologens to CB[8].<sup>6</sup> The complexation of cucurbituril in water, investigated by NMR spectroscopy and ITC, showed a clear switch from 1:1 to 2:1 host/guest stoichiometry on increasing the chain length of the alkyl viologen from 12 to 18 carbon atoms. The formation of the 2:1 host/guest complex is a direct consequence of the inclusion of the viologen unit in

one CB[8] unit and the folding of the longer alkyl chain buried in a second CB[8] hydrophobic cavity. In particular, the unprecedented 2:1 stoichiometry observed in the crystal structure of CB[8] complexed with methyl octadecyl viologen identified 12 as the minimum number of carbon atoms necessary to fill the CB[8] cavity by an aliphatic chain with a U-shaped conformation.<sup>23</sup>

Here, we report for the first time the crystal structure of CB[8] complexed by methyl hexadecyl viologen (MVC16), featuring the unprecedented coexistence of three host–guest complexes with different stoichiometry, namely, 3:2, 2:2, and 1:1, in a highly solvated single crystal.

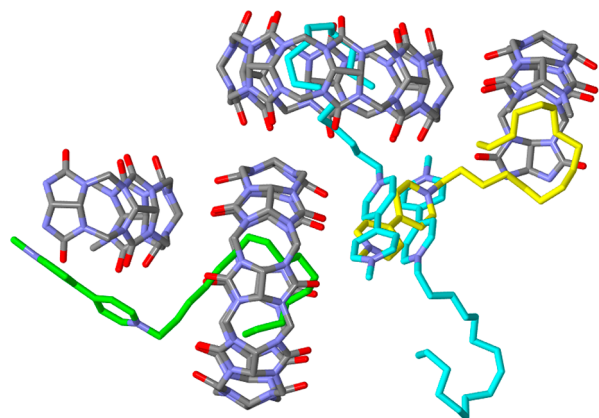


**Figure 1.** Stick representation of the asymmetric unit of CB[8]•MVC16. Hydrogen atoms, water molecules, and counter-anions are omitted for clarity. Two half-molecules of CB[8] are completed by crystallographic inversion symmetry. The overlapped MVC16 molecules, two represented with the carbon atoms in cyan and one in yellow, have 50% occupancy factor.

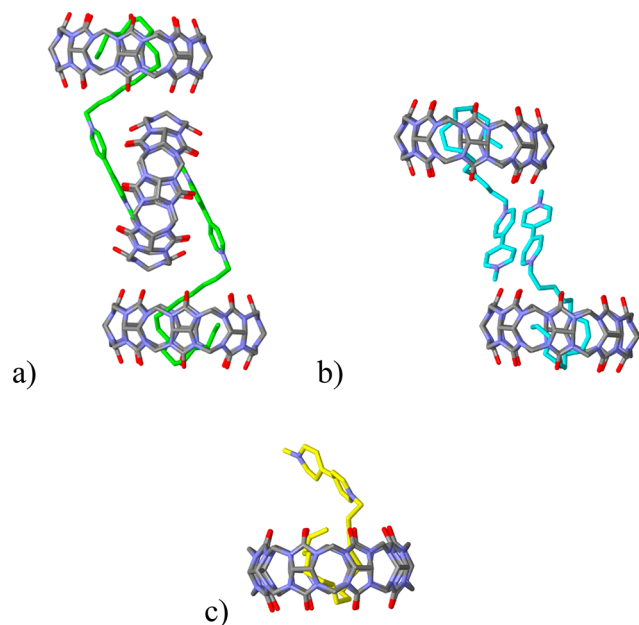


**Figure 2.** Stick representation of the three different host–guest complex units observed in the crystal structure of CB[8]•MVC16: (a) 3:2 CB[8]•MVC16 host–guest complex; (b) 2:2 CB[8]•MVC16 host–guest complex; (c) 1:1 CB[8]•MVC16 host–guest complex. Hydrogen atoms are omitted for clarity.

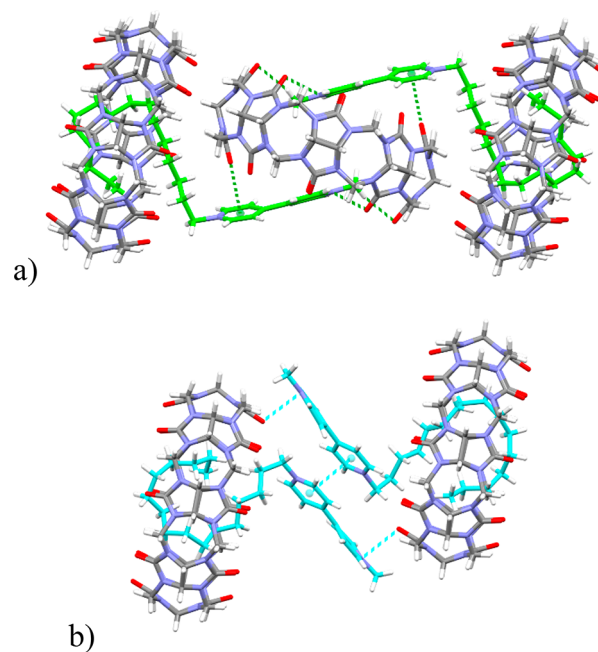


**Figure 3.** Stick representation of the main interactions between CB[8] and MVC16 involving the viologen moiety: (a) 3:2 CB[8]•MVC16 host–guest complex; (b) 2:2 CB[8]•MVC16 host–guest complex.

The light pink, plate single crystals of CB[8]•MVC16 were analyzed by X-ray diffraction using synchrotron radiation and a cryo-cooling technique (100 K). The electron density maps revealed that the asymmetric unit of the triclinic crystal (Figure 1) contains two entire CB[8] molecules located in general positions and two half CB[8] molecules located on crystallographic inversion centers. These macrocycle molecules are complexed by a total of 2.5 MVC16 molecules localized in four different sites, one at full occupancy and three at half-occupancy. The crystal packing shows that MVC16 molecules with partial occupancy are overlapped in various modes. Two independent MVC16 molecules at half-occupancy show  $\pi$ -stacking of the aromatic heads (Figure 1, MVC16 in cyan color), while the same site is also occupied by the aromatic head of the other independent MVC16 molecules at half-occupancy (Figure 1, MVC16 in yellow color). A more complicated overlap involves the aliphatic tails of MVC16 molecules hosted in the CB[8] annuli. The alkyl chain of the MVC16 with partial occupancy, hosted in a centrosymmetric CB[8], overlaps with its inversion related molecule, while the alkyl chains of the other two crystallographically independent MVC16 molecules with partial occupancy are statistically

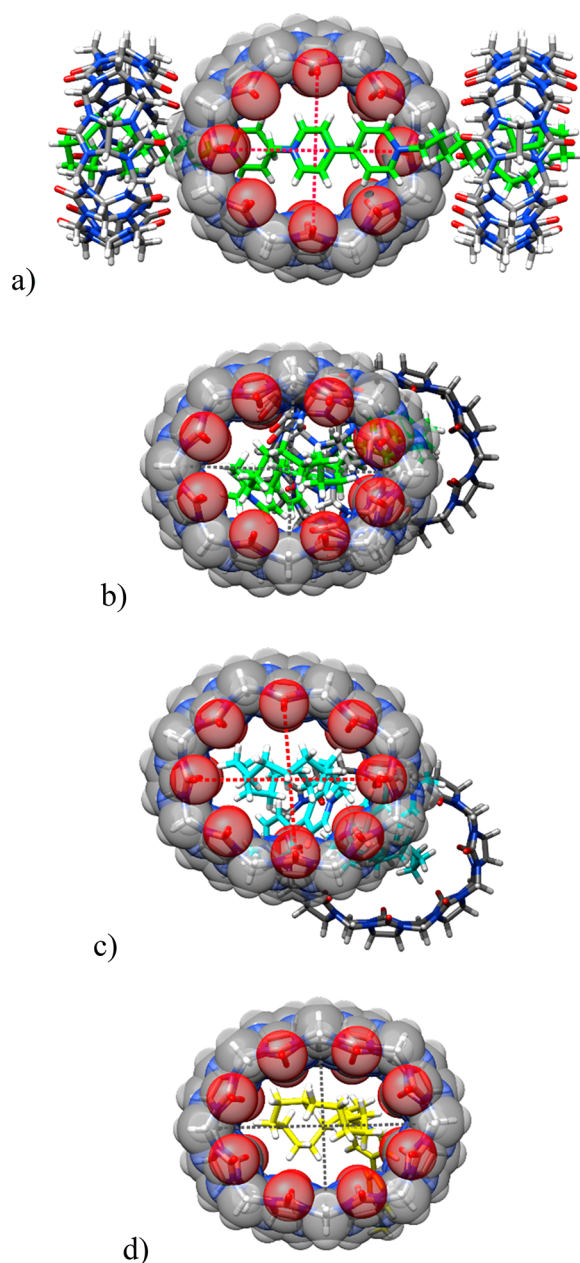


**Figure 4.** Ovalization of the four crystallographically independent **CB[8]** units represented with van der Waals spheres: (a) central and (b) terminal macrorings of 3:2 **CB[8]**•**MVC16** host–guest complex; (c) macroring on the 2:2 **CB[8]**•**MVC16** host–guest complex; (d) macroring of the 1:1 **CB[8]**•**MVC16** host–guest complex. The minor and major axes of the ellipsoidal portal are depicted as dashed lines (C=O...O=C in red, C–H...H–C in black).

hosted by the same asymmetric **CB[8]** with opposite orientation. The overall result is reflected in a very complicated crystal packing of intriguing and complicated interpretation (see below).

The asymmetric unit is completed by five chlorine counterions distributed over 9 sites and about 30 partially disordered water molecules located in the electron density of the remaining potential solvent accessible volume. These solvent-accessible voids correspond to about 30% of the volume of this highly solvated crystal. Residual electron density associated with a further 25 highly disordered water molecules was taken into account in the structure factors by back-Fourier

transformation. Thus, a total of about 55 water molecules can be postulated in the asymmetric unit, consistent with a solvent-accessible volume of 2125 Å<sup>3</sup> and expected volumes of a hydrogen-bonded H<sub>2</sub>O-molecule of 40 Å<sup>3</sup>. Surprisingly, the analysis of the packing indicates the coexistence in the same crystal of three different complex units of **CB[8]**•**MVC16** with 3:2, 2:2, and 1:1 host–guest stoichiometry (Figure 2).

The centrosymmetric 3:2 host–guest complex (Figure 2a) is characterized by a central **CB[8]** molecule, which functions as a dimerization center by hosting the aromatic heads of two **MVC16** guests, while the aliphatic tails are hosted in a hook-like conformation by two other macrocycles. The terminal methyl-pyridinium group of **MVC16** weakly interacts with the carbonyl groups of **CB[8]** through charge–dipole and C–H...O interactions, with the shortest N...O and C...O distances of 3.93 and 3.23 Å, respectively. A hydrogen atom of the methyl group points toward a C=O group of **CB[8]** with H...O distance of 2.40 Å (Figure 3a). The methyl group and the N-pyridinium atom are located inside the cavity at distances from the **CB[8]** carbonyl O-portal planes of 1.24 and 0.39 Å, respectively. The pyridinium mean plane forms an angle of 33.8° with the portal plane. The two pyridinium moieties of the viologen group are mutually rotated by only 19.6°. This conformation allows the formation of another interesting interaction between the second, external aromatic pyridinium group and a carbonyl group of **CB[8]**, which is oriented toward the center of the aromatic ring with a distance of 3.01 Å between the oxygen atom and the ring mean plane (Figure 3a). The two parallel symmetry related pyridinium guests hosted in the central **CB[8]** ring are at a distance of 5.82 Å. The significantly negative electrostatic potential at the portals and within the cavity of **CB[8]** permits the assembly of these two positively charged guests.

For comparison, in the previously reported 2:1 **CB[8]**•**MVC18**, the complexation of the viologen group was completely different.<sup>6</sup> In that case, the viologen moiety was completely inserted into the **CB[8]** cavity with an orthogonal orientation with respect to the portal plane and with the alkyl groups external to the cavity. The partial insertion of the aromatic units observed in the present structure is more reminiscent of that observed in the 1:1 **CB[8]**•**MVC10** complex in which the viologen unit was leaning from the **CB[8]** portal with an angle of about 37°.<sup>18</sup> However, in that case the orientation of the alkyl groups was opposite, with the methyl group external and the decyl group inserted in the ring with a hook-shaped conformation. The typical hook-shaped conformation of the alkyl chain is observed in the complexation of the terminal **CB[8]** hosts. The fourth carbon atom of the hexadecyl chain lies on the carbonyl portal, confirming that 12 is the minimum number of carbon atoms necessary to fill the **CB[8]** cavity. This carbon atom on the portal is in the center of four consecutive trans C–C bonds which links the hook-shaped terminal inserted into the cavity and the initial part of the chain connected to the methyl viologen moiety. The initial N–C and C–C bonds assume torsion angles of about 90°, thereby directing the alkyl chain almost perpendicular to the aromatic unit. The particular conformation of the **MVC16** clips the external **CB[8]** units to the central unit, which results in an overall Z-shaped architecture of the complex with angles between **CB[8]** portals of 85.4° (Figure 2a). The two different host–guest interactions of **CB[8]** units with the inclined methyl viologen and with the hook-shaped alkyl chain observed in this 3:2 complex produce

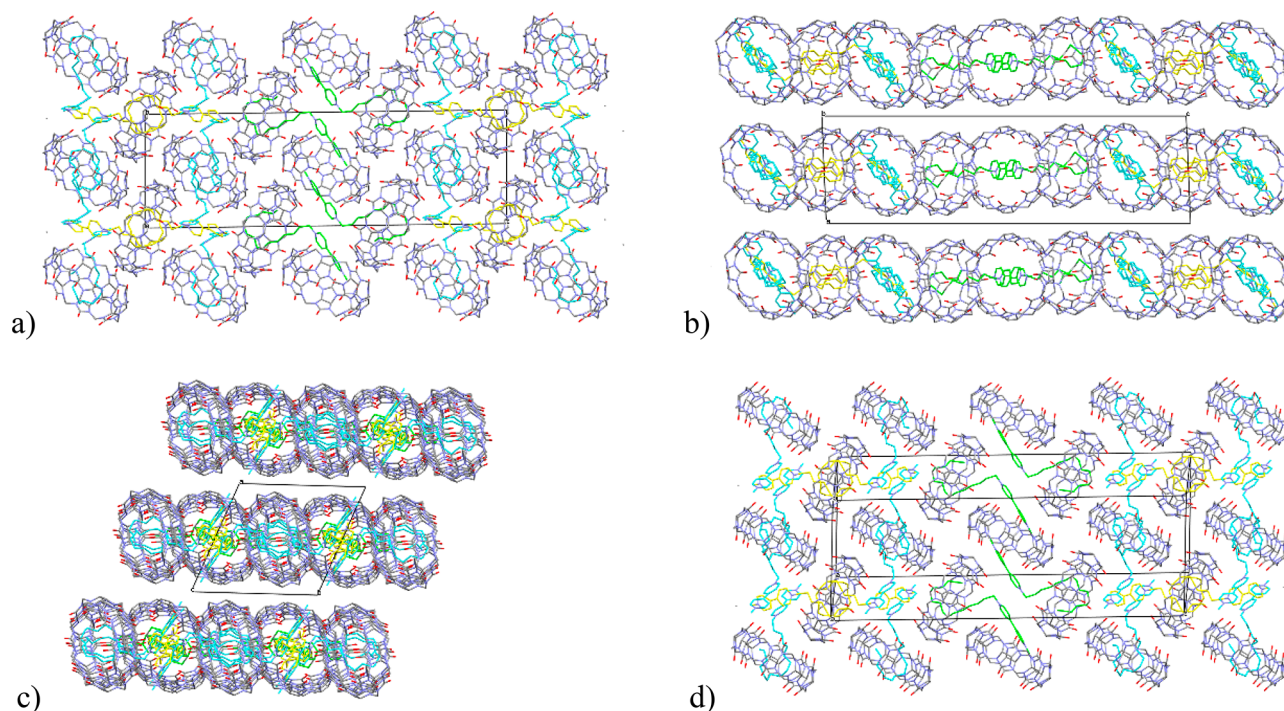


**Figure 5.** Crystal packing viewed along the triclinic cell axes  $a$ ,  $b$ ,  $c$ , (parts a,b,c) and along the reciprocal  $a^*$  axis orthogonal to the  $bc$  plane (d). For clarity, only one layer is represented in d).

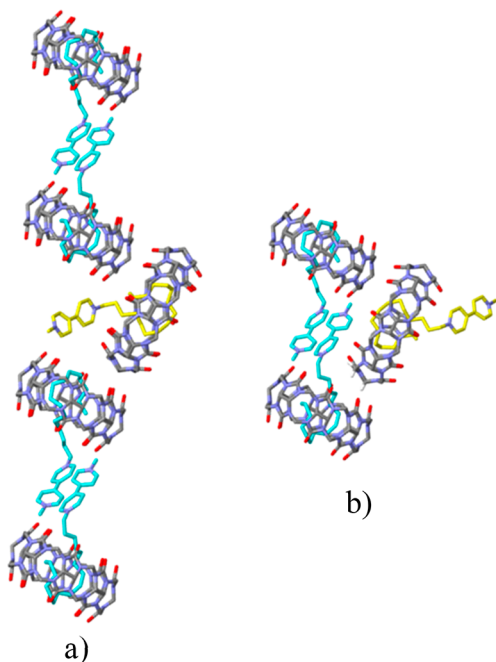


**Figure 6.** Stick representation of the statistical disorder observed in the crystal structure of  $\text{CB}[8]\cdot\text{MVC16}$ . The two alternative dispositions with 0.5 of occupancy factors of the  $\text{MVC16}$  ligand in the 2:2 (cyan) and 1:1 (yellow) complexes are shown in (a) and (b). The  $\text{CB}[8]$  units for these two statistically disordered dispositions (a) and (b) are superimposed, therefore resulting in full occupation of the macrocyclic rings.

two significant different ovalizations of the  $D_{8h}$  symmetric molecule (Figure 4a,b). The difference between the minor and the major axes of the ellipsoidal portal is 1.29 Å for the central  $\text{CB}[8]$ , while the values for the terminal  $\text{CB}[8]$  are 2.94 and 3.26 Å for the internal and external (to the complex) portals,

respectively. In addition, these axes pass through oxygen portal atoms in the case of the central  $\text{CB}[8]$  (Figure 4a), while they pass between adjacent oxygen atoms for the terminal hosts (Figure 4b). This indicates not only a difference in the degree of ovalization, but also a difference in where the  $\text{CB}[8]$  is pinched.

The 2:2 host–guest complex is characterized by the complexation of the terminal aliphatic chains of the  $\text{MVC16}$  inside the  $\text{CB}[8]$  rings with a mutual  $\pi$ -stacking interaction in antiparallel fashion of the viologen moieties (Figure 3b). In particular, the face-to-face stacking interactions involves the pyridinium units connected to the hexadecyl chains with a short distance of 3.56 Å between the two centroids.<sup>24</sup> A long-range electrostatic interaction involves each positively charged N atom of the methyl-pyridinium groups with a carbonyl group of the  $\text{CB}[8]$  which hosts the other  $\text{MVC16}$ , with  $\text{N}\cdots\text{O}$  distances of 3.09 and 3.12 Å (Figure 3b). The layer organization of the crystal packing of  $\text{CB}[8]$  with an open square 2D tiling scheme, in which the parts of the guest molecules external to the macrocycle occupies the interstitial space, is pivotal in the stabilization of the  $\pi$ -stacking interaction between the positively charged groups. In fact, the pyridinium ions are sandwiched between the oxygen portals with negative electrostatic potential (Figure 5). A similar 2:2 complex stabilized by  $\pi\cdots\pi$  interactions between the aromatic moieties of adjacent guests was observed in the crystal structure of  $\text{CB}[8]$  with 1-dodecyl-3-carboxymethylbenzotriazole.<sup>25</sup> In that case, 1:1 host–guest complexes were formed in aqueous solution, while 2:2 host–guest complexes were observed in the solid state by  $\pi\cdots\pi$  dimerization of partially exposed benzotriazole moieties. The conformation of the alkyl chain and the deformation of the  $\text{CB}[8]$  cavity in the present 2:2 complex are similar to that observed in the 3:2 complex. The differences between major and minor ellipsoid axes, which pass through the O atoms, are 2.42 and 2.16 Å for the internal and

external portals, respectively (Figure 4c). The 1:1 complex is characterized by a simple and similar host–guest interaction involving only the MVC16 alkyl tail and the CB[8] unit. This macroring, which lies on a center of crystallographic symmetry, shows an ovalization with a difference in the axes passing between adjacent oxygen atoms of 3.18 Å (Figure 4d). This deformation is very similar to that observed for the terminal CB[8] units of the 3:2 host–guest complex (Figure 4b).

The layer organization of the crystal packing is illustrated in Figure 5. The 2D assembly of the orthogonally oriented CB[8] molecules lies on the *bc* plane of the crystal with a square 2D tiling arrangement (Figure 5d). Each CB[8] molecule interacts in the layer with four orthogonally oriented neighboring CB[8] molecules through extensive C–H...O hydrogen bonds (from 6 to 8 C–H...O distances below the sum of vdW radii for each CB[8]–CB[8] interaction). Each CB[8] molecule acts as an H-donor toward two neighboring CB[8] molecules and as an H-acceptor toward the other two molecules, which partially close the CB[8] portals. There are two similar but distinct types of square cuboid interstitial spaces formed by four neighboring CB[8] molecules. One is filled by the external parts of two viologen moieties involved in 3:2 complexes, related by a crystallographic inversion center. The second is statistically occupied by the heads of the MVC16 moieties involved in 2:2 and 1:1 complexes. The rational interpretation of the electron density maps showing the overlap of this statistical disorder represented an intriguing challenge, not least because both complexes also showed a statistical disorder in the alkyl chains hosted in the CB[8] molecules. The CB[8] of the 1:1 complexes lies on inversion centers, while the two CB[8] units of the 2:2 complexes are related by the translational symmetry along the *b* axis. The two alternate dispositions of the 2:2 and 1:1 complexes, interpreting the 0.50/0.50 statistical disorder, are represented in Figure 6. The overlap of these complexes results in full occupation of the macrocycles. Therefore, the overall crystal structure exhibits the full occupancy of the CB[8] units with alternating chains of 3:2 complexes and 2:2/1:1 complexes packed along one direction of the layer, resulting in a *c*-axis of 52.54 Å (Figure 5d). This peculiar alternation of supramolecular complexes is rather intriguing considering that the driving force responsible for the systematic placing of the guests in a constant CB[8] framework should be minimal.

In conclusion, the highly solvated single crystal of CB[8] complexed by MVC16 shows the unprecedented coexistence of three host–guest complexes with different stoichiometries, namely, 3:2, 2:2, and 1:1. In all complexes the alkyl chain of the MVC16, in the typical hook-shaped conformation, is hosted in the CB[8] macrocycles, while the methyl viologen moieties are differently assembled. In the Z-shaped 3:2 complex, a central CB[8] unit hosts two viologen heads. The 2:2 complex is characterized by a  $\pi$ -stacking interaction between the viologen units. The same sites which favor the dimerization interactions of 2:2 complexes are also statistically occupied by methyl viologen moieties of 1:1 complexes. Therefore, in contrast with the solution behavior dominated by the 2:1 complex, the X-ray structure shows the coexistence of three complexes with different stoichiometry (3:2, 2:2, and 1:1) and architecture, thereby highlighting the fundamental importance of the crystal packing effects in solid-state supramolecular chemistry. The multiple C–H...O interactions between each cucurbituril might reach a level sufficient to stabilize the entire crystal packing.<sup>7</sup> This recalls the concept of

multivalency,<sup>26</sup> in which several carbonyl oxygens of the CB[8] portal can form multiple interactions with the methine and methylene H atoms of neighboring cucurbituril rings. The supramolecular process of crystallization of supramolecular host–guest systems (in other words “supramolecular second order”) involves intermolecular interactions in a small energy window. Therefore, the crystallization process, governed by better directional interactions versus better packing, has permitted us to capture different host–guest systems in a single crystal, revealing a supramolecular landscape in a single photo.

## ■ ASSOCIATED CONTENT

### Supporting Information

The Supporting Information is available free of charge at <https://pubs.acs.org/doi/10.1021/acs.cgd.1c00463>.

Experimental details and X-ray data collection, processing, and refinement statistics (PDF)

### Accession Codes

CCDC 2027429 contains the supplementary crystallographic data for this paper. These data can be obtained free of charge via [www.ccdc.cam.ac.uk/data\\_request/cif](http://www.ccdc.cam.ac.uk/data_request/cif), or by emailing [data\\_request@ccdc.cam.ac.uk](mailto:data_request@ccdc.cam.ac.uk), or by contacting The Cambridge Crystallographic Data Centre, 12 Union Road, Cambridge CB2 1EZ, UK; fax: +44 1223 336033.

## ■ AUTHOR INFORMATION

### Corresponding Author

Silvano Geremia – *Centre of Excellence in Biocrystallography, Department of Chemical and Pharmaceutical Sciences, University of Trieste, 34127 Trieste, Italy*; [orcid.org/0000-0002-0711-5113](https://orcid.org/0000-0002-0711-5113); Email: [sgeremia@units.it](mailto:sgeremia@units.it)

### Authors

Neal Hickey – *Centre of Excellence in Biocrystallography, Department of Chemical and Pharmaceutical Sciences, University of Trieste, 34127 Trieste, Italy*; [orcid.org/0000-0003-1271-5719](https://orcid.org/0000-0003-1271-5719)

Barbara Medagli – *Centre of Excellence in Biocrystallography, Department of Chemical and Pharmaceutical Sciences, University of Trieste, 34127 Trieste, Italy*

Alessandro Pedrini – *Department of Chemistry, Life Sciences and Environmental Sustainability, University of Parma, 43124 Parma, Italy*

Roberta Pinalli – *Department of Chemistry, Life Sciences and Environmental Sustainability, University of Parma, 43124 Parma, Italy*; [orcid.org/0000-0002-0000-8980](https://orcid.org/0000-0002-0000-8980)

Enrico Dalcanale – *Department of Chemistry, Life Sciences and Environmental Sustainability, University of Parma, 43124 Parma, Italy*; [orcid.org/0000-0001-6964-788X](https://orcid.org/0000-0001-6964-788X)

Complete contact information is available at: <https://pubs.acs.org/doi/10.1021/acs.cgd.1c00463>

### Author Contributions

The manuscript was written through contributions of all authors. All authors have given approval to the final version of the manuscript.

### Funding

The authors acknowledge financial support of MIUR through the PRIN project 20179BJNA2.

### Notes

The authors declare no competing financial interest.

## ACKNOWLEDGMENTS

We thank the Elettra Synchrotron (Trieste, Italy) and the staff of the XRD1 beamline for their technical assistance.

## ABBREVIATIONS

CB[8] Cucurbit[8]urils  
MVC16 methyl hexadecyl viologen.

## REFERENCES

- (1) Lagona, J.; Mukhopadhyay, P.; Chakrabarti, S.; Isaacs, L. The Cucurbit[n]uril Family. *Angew. Chem., Int. Ed.* **2005**, *44*, 4844–4870.
- (2) Lee, J. W.; Samal, S.; Selvapalam, N.; Kim, H.-J.; Kim, K. Cucurbituril Homologues and Derivatives: New Opportunities in Supramolecular Chemistry. *Acc. Chem. Res.* **2003**, *36*, 621–630.
- (3) Masson, E.; Ling, X.; Joseph, R.; Kyeremeh-Mensah, L.; Lu, X. Cucurbituril Chemistry: A Tale of Supramolecular Success. *RSC Adv.* **2012**, *2*, 1213–1247.
- (4) Barrow, S. J.; Kasera, S.; Rowland, M. J.; Del Barrio, J.; Scherman, O. A. Cucurbituril-Based Molecular Recognition. *Chem. Rev.* **2015**, *115*, 12320–12406.
- (5) Assaf, K. I.; Nau, W. M. Cucurbiturils: From Synthesis to High-Affinity Binding and Catalysis. *Chem. Soc. Rev.* **2015**, *44*, 394–418.
- (6) Pedrini, A.; Devi Das, A.; Pinalli, R.; Hickey, N.; Geremia, S.; Dalcanele, E. The Role of Chain Length in Cucurbit[8]uril Complexation of Methyl Alkyl Viologens. *Eur. J. Org. Chem.* **2021**, *2021*, 1547–1552.
- (7) Bardelang, D.; Udachin, K. A.; Leek, D. M.; Margeson, J. C.; Chan, G.; Ratcliffe, C. I.; Ripmeester, J. A. Cucurbit[n]urils (n = 5–8): A Comprehensive Solid State Study. *Cryst. Growth Des.* **2011**, *11*, 5598–5614.
- (8) Yang, X.; Wang, R.; Kermagoret, A.; Bardelang, D. Oligomeric Cucurbituril Complexes: from Peculiar Assemblies to Emerging Applications. *Angew. Chem., Int. Ed.* **2020**, *59*, 21280–21292.
- (9) Das, D.; Assaf, K. I.; Nau, W. M. Applications of Cucurbiturils in Medicinal Chemistry and Chemical Biology. *Front. Chem.* **2019**, *7*, 619.
- (10) Pinalli, R.; Pedrini, A.; Dalcanele, E. Biochemical Sensing with Macrocyclic Receptors. *Chem. Soc. Rev.* **2018**, *47*, 7006–7026.
- (11) Correia, H. D.; Chowdhury, S.; Ramos, A. P.; Guy, L.; Demets, G.J.-F.; Bucher, C. Dynamic Supramolecular Polymers built from Cucurbit[n]urils and Viologens. *Polym. Int.* **2019**, *68*, 572–588.
- (12) Cicolani, R. S.; Souza, L. R. R.; de Santana Dias, G. B.; Rocha Gonçalves, J. M.; dos Santos Abrahão, I.; Silva, V. M.; Demets, G.J.-F. Cucurbiturils for Environmental and Analytical Chemistry. *J. Inclusion Phenom. Macrocyclic Chem.* **2021**, *99*, 1–12.
- (13) Combes, S.; Tran, K. T.; Ayhan, M. M.; Karoui, H.; Rockenbauer, A.; Tonetto, A.; Monnier, V.; Charles, L.; Rosas, R.; Viel, S.; Siri, D.; Tordo, P.; Clair, S.; Wang, R.; Bardelang, D.; Ouari, O. Triangular Regulation of Cucurbit[8]uril 1:1 Complexes. *J. Am. Chem. Soc.* **2019**, *141*, 5897–5907.
- (14) Guagnini, F.; Engilberge, S.; Flood, R. J.; Ramberg, K. O.; Crowley, P. B. Metal-Mediated Protein–Cucurbituril Crystalline Architectures. *Cryst. Growth Des.* **2020**, *20*, 6983–6989.
- (15) Zhang, W.; Gan, S.; Vezzoli, A.; Davidson, R. J.; Milan, D. C.; Luzyanin, K. V.; Higgins, S. J.; Nichols, R. J.; Beeby, A.; Low, P. J.; Li, B.; Niu, L. Single-Molecule Conductance of Viologen–Cucurbit[8]uril Host–Guest Complexes. *ACS Nano* **2016**, *10*, 5212–5220.
- (16) Liu, J.; Lambert, H.; Zhang, Y.-W.; Lee, T.-C. Rapid Estimation of Binding Constants for Cucurbit[8]uril Ternary Complexes Using Electrochemistry. *Anal. Chem.* **2021**, *93*, 4223–4230.
- (17) Pazos, E.; Novo, P.; Peinador, C.; Kaifer, A. E.; García, M. D. Cucurbit[8]uril (CB[8])-Based Supramolecular Switches. *Angew. Chem., Int. Ed.* **2019**, *58*, 403–416.
- (18) Ko, Y. H.; Hwang, I.; Kim, H.; Kim, Y.; Kim, K. Molecular pop-up toy: A Molecular Machine Based on Folding/Unfolding Motion of Alkyl Chains Bound to a Host. *Chem. - Asian J.* **2015**, *10*, 154–159.
- (19) Fang, X.; Kögerler, P.; Isaacs, L.; Uchida, S.; Mizuno, N. Cucurbit[n]uril#Polyoxoanion Hybrids. *J. Am. Chem. Soc.* **2009**, *131*, 432–433.
- (20) Wu, G.; Olesińska, M.; Wu, Y.; Matak-Vinkovic, D.; Scherman, O. A. Mining 2:2 Complexes from 1:1 Stoichiometry: Formation of Cucurbit[8]uril-Diarylvologen Quaternary Complexes Favored by Electron-Donating Substituents. *J. Am. Chem. Soc.* **2017**, *139*, 3202–3208.
- (21) Wu, G.; Szabó, I.; Rosta, E.; Scherman, O. A. Cucurbit[8]uril-Mediated Pseudo[2,3]rotaxanes. *Chem. Commun.* **2019**, *55*, 13227–13230.
- (22) Xiao, X.; Sun, N.; Qi, D.; Jiang, J. Unprecedented Cucurbituril-Based Ternary Host-Guest Supramolecular Polymers Mediated through Included Alkyl Chains. *Polym. Chem.* **2014**, *5*, 5211–5217.
- (23) Ko, Y. H.; Kim, H.; Kim, Y.; Kim, K. U-Shaped Conformation of Alkyl Chains Bound to a Synthetic Host. *Angew. Chem., Int. Ed.* **2008**, *47*, 4106–4109.
- (24) Janiak, C. A. Critical Account on  $\pi$ - $\pi$  Stacking in Metal Complexes with Aromatic Nitrogen-containing Ligands. *J. Chem. Soc., Dalton Trans.* **2000**, 3885–3896.
- (25) Zhang, P.-Q.; Wang, C.-C.; Liu, P.-P.; Xiao, X.; Ma, D.; Li, Z.-T.; Yang, B. Supramolecular Assemblies Constructed from Cucurbit[8]uril and N-alkyl Carboxymethylbenzotriazole through Host-Guest Interactions. *ChemistrySelect* **2020**, *5*, 12477.
- (26) Badjic, J. D.; Nelson, A.; Cantrill, S. J.; Turnbull, W. B.; Stoddart, J. F. Multivalency and Cooperativity in Supramolecular Chemistry. *Acc. Chem. Res.* **2005**, *38*, 723–732.